Int. J. Heat Mass Transfer. Vol. 13, pp. 725–739. Pergamon Press 1970. Printed in Great Britain

SURFACE ROUGHNESS EFFECTS ON RADIANT TRANSFER BETWEEN SURFACES*

R. G. HERING† and T. F. SMITH‡

Department of Mechanical and Industrial Engineering, University of Illinois at Urbana-Champaign, Urbana, Illinois, U.S.A.

(*Received* 14 *July* 1969)

Abstract—Radiative heat transfer between opaque interacting surfaces is formulated for equal temperature adjoint plates with a one-dimensional surface roughness profile. The rough surface bidirectional reflectance and directional emittance introduced in the analysis depend on material emittance, roughness element specularity and surface roughness slope. Numerical solutions to the giverning integral equation for radiant intensity yields local and total heat transfer for a range of each of the rough surface parameters. The heat transfer results indicate that roughness effects are relatively unimportant for high emittance materials while for low emittance materials roughness slope can change local flux and total radiant heat transfer by a factor of two. Comparison of rough surface heat transfer to that evaluated with simple surface property models demonstrates the superiority of the diffuse emission–diffuse reflection model employing rough surface apparent hemispherical emittance. The error incurred in local flux using this simple model, however, can be significant.

NOMENCLATURE

dA, plate surface area element [ft^2];
H, intensity ratio, I^+/I_b [dimensionless];
I^+, I^-, intensities of emergent and incident energies [Btu/hft^{2}sr];
I_b, intensity of black surface at plate temperature [Btu/hft^{2}sr];
l, plate length [ft];
q, local radiant flux [Btu/hft^2];
Q, total radiant heat transfer rate [Btu/h];
T, plate temperature [°R];
x, y, z, coordinates on plates [ft];
α, α_w, apparent directional and wall absorptance [dimensionless];
γ, included angle between plates [deg.];
Δ_{ij}, angular difference function [dimensionless];
δ, Dirac delta function [dimensionless];
$\varepsilon, \varepsilon_a, \varepsilon_H, \varepsilon_w$, apparent directional, apparent hemispherical, hemispherical and wall emittance [dimensionless];
θ, θ', angles of emergent and incident energies [deg.];
θ'_{lim}, limiting angle of incident energy [deg.];
Θ, angle of emergent energy defined in equation (9) [deg.];
ξ, η, relative plate coordinates x/l and y/l [dimensionless];
$\rho^S_{bd}, \rho^D_{bd}, \rho_{bd}$, specular component, diffuse component, total bidirectional reflectance [sr^{-1}];
$\rho^S_w, \rho^D_w, \rho_w$, specular component, diffuse component, total wall reflectance [dimensionless];

* This paper presents results of research supported in part by Jet Propulsion Laboratory, California Institute of Technology, Contract 951661.

† Professor.

‡ Research Assistant.

σ, Stefan–Boltzmann radiation constant [Btu/hft^2 °R^4];
χ, roughness included angle [deg.];
$d\omega, d\omega'$, solid angle increments of emergent and incident energies [sr].

INTRODUCTION

RADIATIVE energy transfer among interacting opaque surfaces is generally evaluated with radiation property models which postulate that emission is diffuse and reflection is either diffuse or specular. It is well known, however, that many engineering materials exhibit properties which do not conform to these simple models. Surface topography is one of the characteristics of surfaces which contributes to the differences between real surface radiation properties and the property models of analysis. Roughness influences both the amount of energy emitted and reflected relative to that of the constituent material as well as the spatial distribution of these energies. Since the methods employed to evaluate radiant transfer generally do not account for such effects, these techniques may lead to significant differences between predicted and observed radiative heat transfer rates. Definitive studies establishing the influence of surface roughness on radiative transfer are lacking. Furthermore, little is known concerning the magnitude of the error incurred when such real surface characteristics are neglected and simple property models are employed. Recently [1], all apparent thermal radiation properties required to implement studies of surface roughness effects on radiative transfer were reported for a one-dimensionally rough surface. It is the purpose here to utilize the apparent properties to assess the importance of surface roughness on radiative transfer between interacting surfaces and to evaluate the magnitude of the discrepancy in heat flux incurred when simple property models are used.

Studies of radiant energy transfer for interacting non-black surfaces which account for a spatial distribution of reflected energy which is neither specular nor diffuse are limited. Heat transfer between uniform temperature semi-infinite parallel plates [2] and some simply arranged plane surfaces [3] has been reported utilizing the Beckmann bidirectional reflectance model [4]. This model is based on diffraction theory and is applicable to slightly rough metallic surfaces. These studies indicated that the reflectance model employed in the analysis of radiant transfer influenced local and overall radiant energy interchange rates to a greater

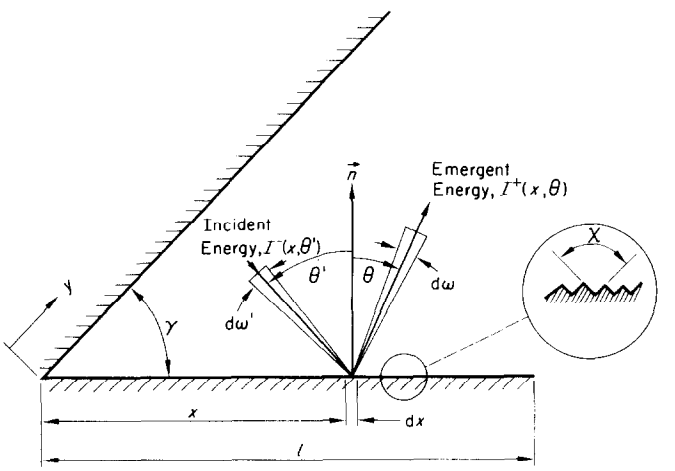

FIG. 1. Schematic diagram of adjoint plate system.

degree than radiant heat transfer rates. Differences in local irradiation values greater than a factor of three were observed between that predicted with simple property models and that evaluated using the detailed bidirectional reflectance model. Similar observations were made by Wilden and Treat [5] who employed a modified form [6] of the bidirectional reflectance model proposed by Torrance and Sparrow [7]. Studies of radiant interchange between a black surface and a parallel surface with one-dimensional grooves [8–10] illustrated the large effects directional radiative properties produce on energy interchange.

The system of interacting surfaces selected for study consists of equal length plates of infinite width sharing a common edge and including angle γ (see Fig. 1). Both surfaces have identical uniform temperature and radiative properties. This simple configuration was chosen primarily because of the availability of extensive radiant heat transfer results [11–13] evaluated on the basis of the simple direction independent property models commonly employed in radiant heat-transfer analysis. The surface roughness of each plate consists of V-groove elements of identical included angle with axes parallel to that of the adjoint plates. The apparent thermal radiation properties for the surface roughness contour described have been developed in [1]. External sources of radiant energy are absent and the intervening media is radiatively non-participating.

ANALYSIS

Radiant transfer formulation

Consider differential surface area element dA $(=dx\,dz)$ located at distance x from the common edge of the plates. Let θ denote an arbitrary direction measured from the mean surface normal in a plane normal to the plate axis. The radiant energy emerging from the considered plate increment per unit time and per unit area which is confined to the solid angle increment $d\omega$ defined by the cylindrical sector subtended by angular increment $d\theta$ is

$$\frac{\pi}{2} I^+(x, \theta) \cos\theta \, d\theta. \tag{1}$$

$I^+(x, \theta)$ denotes the local radiant intensity at location x in direction θ and the solid angle relation $d\omega = \pi\, d\theta/2$ has been employed. This emerging energy consists of emission and of incident energy which after reflection from the surface exits within the considered solid angle. The energy emitted per unit time and per unit area by the element into $d\omega$ is

$$\frac{\pi}{2} \varepsilon(\theta)\, I_b \cos\theta \, d\theta \tag{2}$$

where $\varepsilon(\theta)$ is the apparent directional emittance of the surface and I_b is the space and direction independent intensity of a black surface evaluated at the plate temperature. To formulate the contribution of reflected energy to that emerging within $d\omega$, consider first the radiant energy incident on dA from within the solid angle increment $d\omega'$ defined by the angular increment $d\theta'$ about direction θ'. Let the intensity of incident energy at location x for direction of incidence θ' be designated $I^-(x, \theta')$. Then the energy incident on dA per unit time and per unit area from the solid angle $d\omega'$ about the θ' direction is

$$\frac{\pi}{2} I^-(x, \theta') \cos\theta' \, d\theta'. \tag{3}$$

The portion of unit incident energy which emerges within $d\omega$ after reflection from the opaque rough surface is

$$\frac{\pi}{2} \rho_{bd}(\theta', \theta) \cos\theta \, d\theta \tag{4}$$

where $\rho_{bd}(\theta', \theta)$ denotes the apparent bidirectional reflectance of the rough surface. Hence, the contribution of energy incident within $d\omega'$ to that emerging within $d\omega$ follows as

$$\left(\frac{\pi}{2}\right)^2 \rho_{bd}(\theta', \theta)\, I^-(x, \theta') \cos\theta' \cos\theta \, d\theta' \, d\theta. \tag{5}$$

To account for all possible directions of incident energy which can contribute to the energy

emerging in the θ direction requires integration of equation (5) over direction of incidence.

$$\left(\frac{\pi}{2}\right)^2 \cos\theta \, d\theta \int_{-\pi/2}^{\pi/2} \rho_{bd}(\theta', \theta) \, I^-(x, \theta') \cos\theta' \, d\theta'. \quad (6)$$

Equating equation (1) to the sum of equations (2) and (6) yields

$$I^+(x, \theta) = \varepsilon(\theta) \, I_b + \frac{\pi}{2} \int_{-\pi/2}^{\pi/2} \rho_{bd}(\theta', \theta) \, I^-(x, \theta') \times \cos\theta' \, d\theta'. \quad (7)$$

For the adjoint plate system in the absence of external radiation fields, the contributing directions of incident energy are limited to a value $\theta'_{\text{lim}}(x)$ less in absolute value than $\pi/2$ and given by

$$\theta'_{\text{lim}}(x) = -\tan^{-1}\left[\frac{\cos\gamma - (x/l)}{\sin\gamma}\right]. \quad (8)$$

Also, since the intervening medium between the surfaces is radiatively transparent, the intensity of incident energy $I^-(x, \theta')$ is identical to the intensity of emergent energy of the adjacent plate evaluated at a suitable location and direction, $I^+(y, \Theta)$. From geometry it follows that

$$\left.\begin{aligned} y/x &= \cos\theta'/\cos(\theta' - \gamma) \\ \Theta &= \theta' - \gamma \end{aligned}\right\}. \quad (9)$$

Hence, equation (7) may be written

$$I^+(x, \theta) = \varepsilon(\theta) \, I_b + \frac{\pi}{2} \int_{\theta_{\text{lim}}(x)}^{\pi/2} \rho_{bd}(\theta', \theta) \, I^+(y, \Theta) \times \cos\theta' \, d\theta'. \quad (10)$$

Note that y and Θ do not constitute additional independent variables since according to equation (9) they are completely specified in terms of x and θ'. As a result of the symmetry in the system, the intensity to the left and that within the integral operator refer to the identical physical quantity. Thus, equation (10) constitutes a linear integral equation for the angular dependence of local radiant intensity. Equation (10) may be expressed in the following dimensionless form

$$H(\xi, \theta) = \varepsilon(\theta) + \frac{\pi}{2} \int_{\theta_{\text{lim}}(\xi)}^{\pi/2} \rho_{bd}(\theta', \theta) \, H(\eta, \Theta) \times \cos\theta' \, d\theta' \quad (11)$$

where the dimensionless intensity $H(\xi, \theta)$ and distance coordinates ξ and η are

$$H(\xi, \theta) = \frac{I^+(x, \theta)}{I_b}, \quad \xi = \frac{x}{l}, \quad \eta = \frac{y}{l}. \quad (12)$$

Once the local radiant intensity has been evaluated, local radiant heat transfer rate $q(x)$ follows from the difference between the rates at which radiant energy emerges from and arrives at the considered element. In dimensionless form

$$\frac{q(\xi)}{\sigma T^4} = \frac{1}{2} \int_{-\pi/2}^{\pi/2} H(\xi, \theta) \cos\theta \, d\theta - \frac{1}{2} \int_{\theta_{\text{lim}}(\xi)}^{\pi/2} H(\eta, \Theta) \times \cos\theta' \, d\theta. \quad (13)$$

Alternatively, dimensionless local radiant heat transfer may be expressed as the difference between emission rate and rate of absorption of incident energy.

$$\frac{q(\xi)}{\sigma T^4} = \varepsilon_a - \frac{1}{2} \int_{\theta_{\text{lim}}(\xi)}^{\pi/2} \alpha(\theta') \, H(\eta, \Theta) \cos\theta' \, d\theta'. \quad (14)$$

The symbols ε_a and $\alpha(\theta')$ denote apparent hemispherical emittance and apparent directional absorptance of the rough surface, respectively.

Total radiant heat transfer from each plate per unit depth and black surface emissive power is obtained by integration of equation (14) over the extent of the surface. Thus,

$$\frac{Q/l}{\sigma T^4} = \int_0^1 \frac{q(\xi)}{\sigma T^4} \, d\xi. \quad (15)$$

It is evident from equations (11) and (13) that radiant transfer is influenced by the rough surface properties $\rho_{bd}(\theta', \theta)$ and $\varepsilon(\theta)$. These properties are briefly described in the following section in order to facilitate interpretation of the heat-transfer results presented later.

Rough surface radiation properties

All apparent radiation properties for a one-dimensionally rough surface consisting of symmetric V-shaped roughness elements with identical included angle have been reported [1]. In the cited study asperity walls were diffusely emitting with wall emittance (ε_w) equal to wall absorptance (α_w). A direction independent reflectance model with a specular component (ρ_w^S) and a diffuse component (ρ_w^D) was employed to describe reflection within roughness elements. In addition to the material properties, the apparent radiation properties depend on included angle of the roughness element χ. Alternatively, the included angle dependence may be viewed as a dependence on surface roughness slope. The influence of the aforementioned parameters on bidirectional reflectance is presented in terms of wall absorptance α_w, wall specularity parameter ρ_w^S/ρ_w, and included angle χ. It is not the purpose here to discuss the property results at length, but rather to point out some important characteristics of the rough surface bidirectional reflectance pertinent to the present study. Other rough surface properties are presented and discussed elsewhere [1].

Bidirectional reflectance is expressed as the sum of a specular component $\rho_{bd}^S(\theta', \theta)$ and a diffuse component $\rho_{bd}^D(\theta', \theta)$. The specular component accounts for incident energy which undergoes only specular interreflections within surface asperities before emerging from the surface. It may be expressed in terms of direction dependent reflectance factors $\rho_{ij}(\theta')$, direction of leaving energy θ, and angular difference functions $\Delta_{ij}(\theta)$ as

$$\rho_{bd}^S(\theta', \theta) = \frac{2}{\pi} \sum_{i=1}^{2} \sum_{j=1}^{2} \frac{\rho_{ij}(\theta')}{\cos \theta} \delta [\theta' - \Delta_{ij}(\theta)] \tag{16}$$

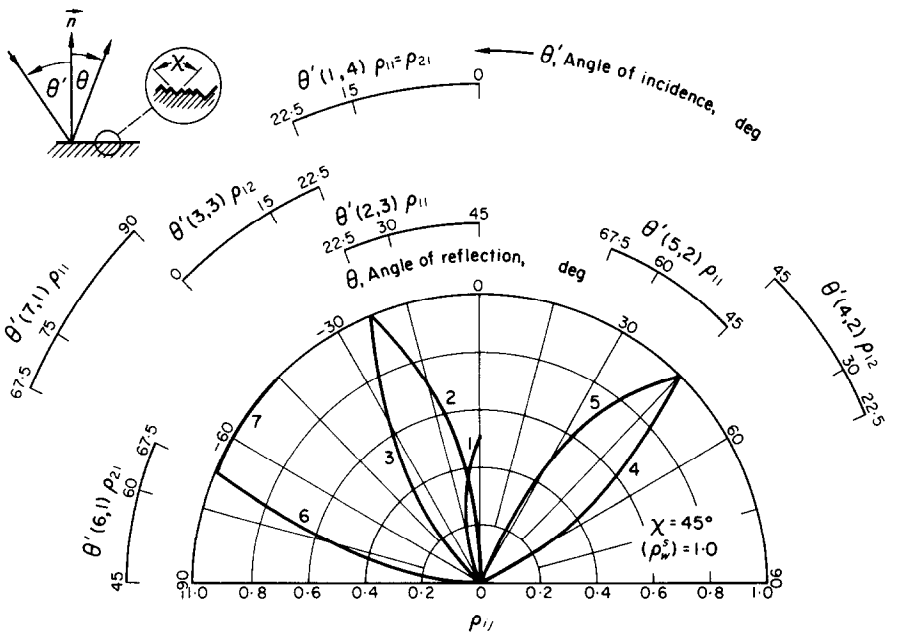

FIG. 2. Specular reflectance factors ($\chi = 45°$, $\rho_w^S = 1{\cdot}0$).

where δ is the Dirac delta function. In addition to the direction of incident energy, reflectance factors depend on χ and ρ_w^s. Typical results for $\rho_{ij}(\theta')$ are illustrated in Fig. 2 for an included angle χ of 45° and $\rho_w^s = 1{\cdot}0$. The most significant feature clearly evident in the figure is the dominant role played by back-scattering which is indicated by a sign reversal between the direction of incident and reflected energy. A back-scattered beam is present for all directions of incident energy and a forward-scattered beam only exists for a limited range of direction for incident energy. For an included angle of 90° [1] a forward-scattered beam does not exist for any direction of incident energy. Clearly, the specular component of bidirectional reflectance for the rough surface displays characteristics grossly different from that exhibited by property models commonly employed in radiant transfer analysis.

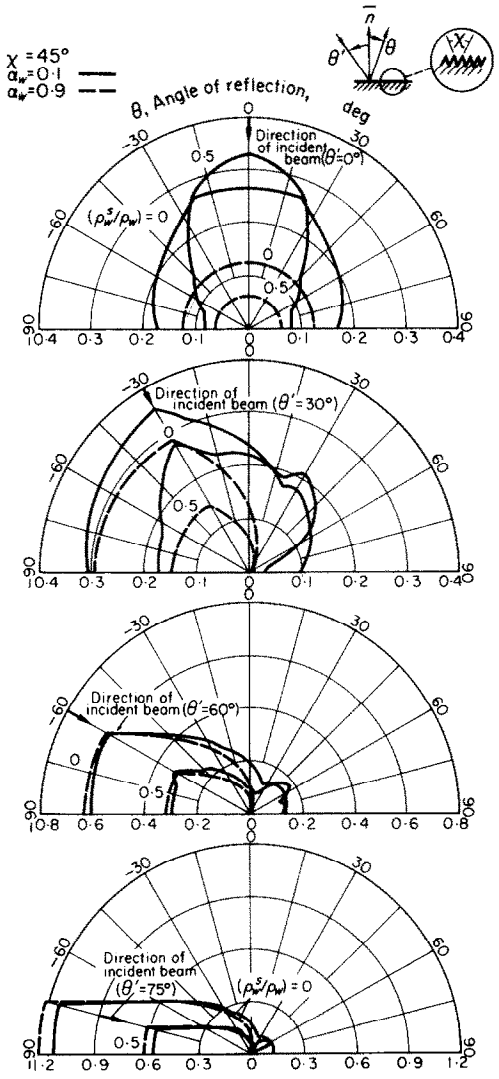

FIG. 3. Diffuse component of bidirectional reflectance ($\chi = 45°$) (divide ρ_{bd}^D values read from figure by 10 for $\alpha_w = 0{\cdot}9$).

The diffuse bidirectional reflectance component $\rho_{bd}^D(\theta', \theta)$ accounts for energy incident from the θ' direction which undergoes at least one diffuse reflection within a surface asperity before exiting from the surface. The expression developed is lengthy and requires numerical evaluation; therefore, it is not presented here. Typical results for $\rho_{bd}^D(\theta', \theta)$ are presented in Fig. 3 for a groove included angle 45° and wall absorptance values of 0·1 and 0·9 for directions of incident energy of 0°, 30°, 60° and 75°. In each portion of the figure distributions are illustrated for wall specularity ratios corresponding to diffuse ($\rho_w^S/\rho_w = 0$) and diffuse-specular ($\rho_w^S/\rho_w = 0{\cdot}5$) walls. The most striking features of the results are the gross departure of the distributions from those of a diffusely reflecting plane surface especially at moderate to large angles of incidence and the concentration of reflected energy into directions near that of the incident beam. A nearly diffuse distribution of reflected energy is only found at normal incidence and large wall absorptance. The general characteristics of $\rho_{bd}^D(\theta', \theta)$ do not change appreciably when included angle is increased to 90°. Again, the apparent properties of the rough surface differ significantly from the surface property models of engineering radiant transfer analysis. Back-scattering is also dominant in the diffuse bidirectional reflectance component.

The bidirectional reflectance model for the rough surface may be introduced into equation

(11) and the following result obtained

$$H(\xi,\theta)=\varepsilon(\theta)+\sum_{i=1}^{2}\sum_{j=1}^{2}\rho_{ij}\left[\Delta_{ij}(\theta)\right]\frac{\cos\left[\Delta_{ij}(\theta)\right]}{\cos\theta}\times H\left[\eta\left\{\xi,\theta_{ij}\right\},\Theta\left\{\Delta_{ij}\right\}\right]+\frac{\pi}{2}\int_{\theta_{\lim}(\xi)}^{\pi/2}\times\rho_{bd}^{D}(\theta',\theta)\,H(\eta,\Theta)\cos\theta'\,\mathrm{d}\theta'. \quad (17)$$

METHOD OF SOLUTION

Since only numerical results were available for the diffuse component of bidirectional reflectance, numerical techniques were employed to solve the integral equation governing dimensionless local radiant intensity. The continuous space domain was replaced with N discrete equidistant space points ξ_i. At each space point, equal angular increments about n discrete directions were selected. Standard quadrature formulae were used to replace the integral in equation (17) with the sum of view factor-intensity products. The result of this procedure is a system of $n \times N$ simultaneous linear algebraic equations. These were solved by a successive substitution method with the initial dimensionless intensity estimates given by apparent directional emittance. The numerical procedure was verified by calculating heat flux for diffusely emitting surfaces with either diffuse or specular reflection and comparing these results with those available in the literature [11, 12]. Except for a small oscillation (maximum value less than 1 per cent) for specularly reflecting surfaces in some instances, computed local heat flux values were indistinguishable from those determined by earlier investigators when employing $N = 50$ and $n = 36$. Rough surface heat flux results obtained for larger values for N and n showed no perceptible change from those determined for the above cited values. As a result of these numerical experiments, it is conservatively estimated that the results are accurate to at least 1 per cent for local flux and are of even greater precision for total heat transfer.

RESULTS AND DISCUSSION

Local radiant flux

Dimensionless radiant heat flux distributions are illustrated in Figs. 4 and 5 for an included angle of 45° between the plates. Results are presented for wall emittance values 0·1, 0·5 and 0·9 for diffusely reflecting ($\rho_w^S/\rho_w = 0$) and specularly reflecting ($\rho_w^S/\rho_w = 1{\cdot}0$) surface asperities. Distributions for roughness element included angle of 45° are shown in Fig. 4 and for included angle of 90° in Fig. 5. The general characteristics of the flux distributions follow expected trends [11, 13]. Flux monotonically increases with distance from the apex and its uniformity increases and level diminishes as wall emittance is decreased.

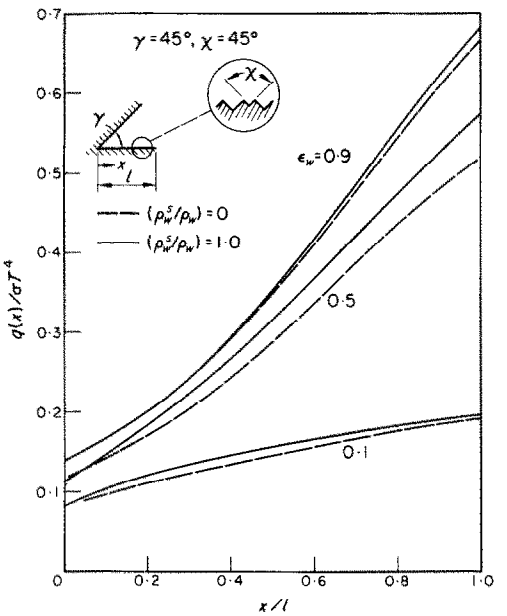

FIG. 4. Dimensionless radiant heat flux distribution ($\gamma = 45°$, $\chi = 45°$).

According to Fig. 4 local flux is greater for specularly reflecting roughness elements than for diffusely reflecting walls for each wall

emittance value. Flux differences are small, however, when emittance is large and generally less than 10 per cent for the intermediate and low wall emittance values. The greater local flux values observed for specularly reflecting grooves is attributed to the forward scattering of energy by the specular component of bidirectional reflectance. In contrast, local flux is greater for diffusely reflecting surface asperities when roughness slope is diminished by increasing roughness included angle to 90° as shown in Fig. 5. Again, flux differences are small for large emittance elements, but now these differences increase significantly as emittance is reduced. Local flux for diffuse walls attain values as large as 50 per cent greater than that for specular walls at the low emittance value. The lower flux for specularly reflecting roughness elements is attributed to the lack of any significant amount of scattering of energy out the opening by the specular component of bidirectional reflectance when $\chi = 90°$.

Comparison of flux distributions in Figs. 4 and 5 affords an opportunity to observe the influence of surface topography on local flux. It is apparent from the results displayed that when all other roughness parameters are identical, the surface with larger roughness slope experiences greater heat flux levels. While flux differences are small for large wall emittance, they increase with decreasing wall emittance until at low emittance, flux for the surface of larger slope attains values which exceed by a factor of two those for the surface of smaller slope. The flux differences are attributed to the greater increase in apparent emittance over wall emittance for the surface with larger roughness slope; an increase which is enhanced as wall emittance is diminished. Roughness slope affects the results for specularly reflecting asperities to a greater degree than those for diffusely reflecting walls. This influence may be readily interpreted in terms of the characteristics of the bidirectional reflectance model appropriate to the surfaces of different roughness slope. As mentioned earlier, the diffuse components of bidirectional reflectance for both roughness slopes do not differ significantly in their overall characteristics. On the other hand, the specular components of bidirectional reflectance for the two surfaces differ in one important characteristic. While both yield back-scattering of energy for all directions of incident energy, the specular bidirectional reflectance component for the surface with larger roughness slope also possesses a strong forward scattering contribution. Hence, all other conditions being identical, the surface with smaller roughness slope offers significantly greater impedance to energy flow out the opening and, consequently, experiences considerably less heat transfer. For example, local flux at the midpoint for $\varepsilon_w = 0{\cdot}1$ and $\chi = 45°$ is approximately 40 per cent greater than that for $\chi = 90°$ and the same wall emittance when the groove walls are diffusely reflecting. A similar comparison for specularly reflecting walls shows that the surface of larger roughness slope experiences a heat transfer rate twice as large as that for the surface with smaller roughness slope.

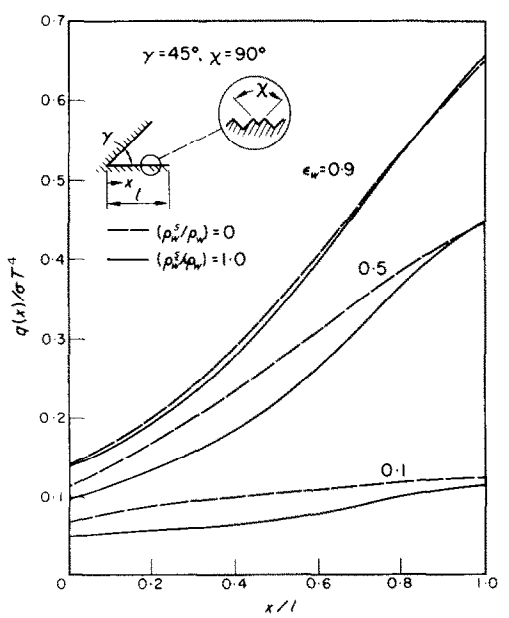

FIG. 5. Dimensionless radiant heat flux distributions ($\gamma = 45°$, $\chi = 90°$).

Of particular interest is a comparison of rough surface heat flux to that evaluated using radiation surface property models commonly employed in engineering analysis. Results obtained by using the diffuse emission–diffuse reflection model which ignores directional dependence of properties are denoted CD (constant diffuse). If reflection is considered specular, the corresponding results are denoted CS (constant specular). Some results are also presented for a compromise model which accounts for the surface apparent emittance ε_a. Constant property results based on wall emittance completely neglect the influence of roughness on surface properties and, hence, heat transfer. Constant property results obtained using apparent emittance account for the influence of surface roughness on the magnitude of energy emission and reflection, but disregard roughness influences on the spatial distribution of emitted and reflected energy. Directional diffuse analysis employed apparent hemispherical emittance

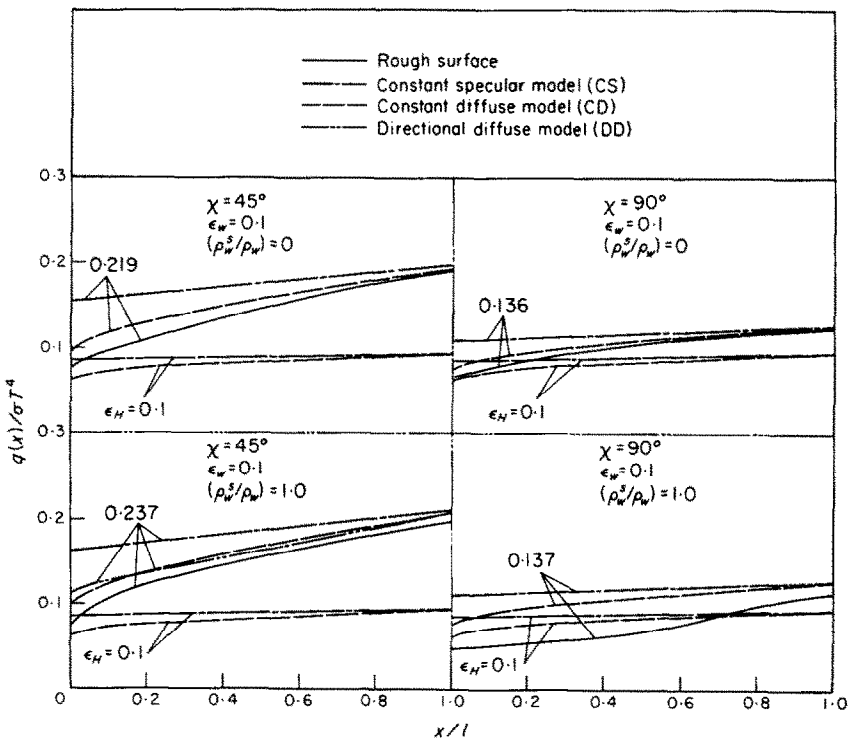

FIG. 6. Comparison of rough surface heat flux to results from simple property models ($\varepsilon_w = 0{\cdot}1$).

directional dependence of rough surface emittance and reflectance, but assumes reflected energy to be diffusely distributed. Results for this model are designated DD (directional diffuse). Distributions were obtained for the direction independent property models employing hemispherical emittance values ε_H given by rough surface wall emittance ε_w and rough with directional emittance and reflectance evaluated with the rough surface distributions. Thus, in addition to accounting for roughness effects on total emission and reflection, DD results partially account for the directional dependence in the rough surface properties.

Dimensionless radiant flux distributions evaluated from the rough surface analysis as

well as from the less detailed analysis required for the simpler property models mentioned above are presented in Fig. 6 for $\varepsilon_w = 0{\cdot}1$. Local flux values which are in error by a factor of two are clearly evident when surface roughness is completely ignored. Except for specularly reflecting roughness elements with 90° included angle, the error in constant property results is markedly reduced when the influence of roughness on emittance and reflectance is accounted for by utilizing rough surface apparent emittance in the constant property calculation. Furthermore, the results shown for the constant property models clearly establish the superiority of the diffuse reflection model. This is not surprising in view of the fact that the specular reflection model exhibits only forward-scattering of energy while with the diffuse model back-scattering does occur. Although the CD results employing the rough surface apparent emittance yield the best approximation to the rough surface flux distributions, the discrepancy in flux values is not everywhere negligible. At the apex where the maximum discrepancy occurs, flux differences vary from almost 18 per cent for diffuse cavity walls with 90° included angle to 35 per cent cent for specularly reflecting asperities of 45° included angle. The simple diffuse model yields the most accurate results in the exceptional case cited earlier ($\chi = 90°$, $\rho_w^S/\rho_w = 1{\cdot}0$) when wall emittance rather than apparent emittance is utilized. This may be attributed to the fact that the lower wall emittance simply shifts CD results to lower values while the flux distribution remains decidedly different from that of the rough surface. Flux distributions evaluated with the DD model were almost indistinguishable from those for the CD model with $\varepsilon_H = \varepsilon_a$. A typical result is illustrated. The lack of any significant improvement with DD analysis is testimonial to the dominant role played by back-scattering reflection phenomena on the heat transfer process.

Local flux distributions are presented in Fig. 7 for $\varepsilon_w = 0{\cdot}5$. As a consequence of the conclusions drawn from the low wall emittance

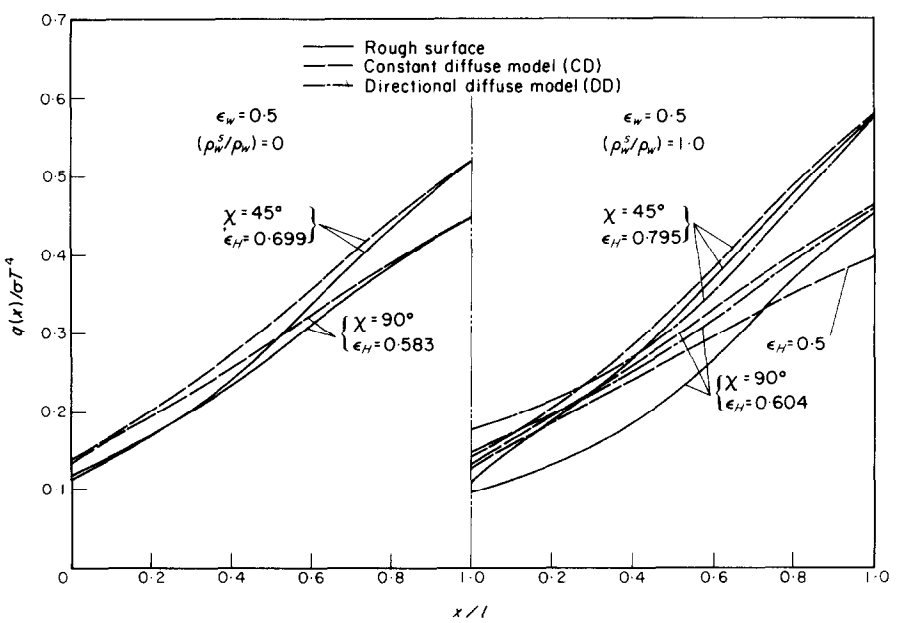

FIG. 7. Comparison of rough surface heat flux to results from simple property models ($\varepsilon_w = 0{\cdot}5$).

results, distributions are generally limited to the CD model and the DD model employing rough surface apparent hemispherical emittance. The maximum error incurred with the CD model is at the apex and varies from approximately 14 per cent for diffuse roughness elements to almost 50 per cent for specular surface asperities. Some improvement is again noted in the exceptional situation noted earlier when wall emittance is employed in CD analysis. Results from DD analysis are not shown for the rough surface with diffusely reflecting asperities because they differ imperceptibly from the CD distributions. DD results at the apex are significantly poorer than those of CD analysis for specularly reflecting roughness elements. According to Fig. 8, CD analysis using rough surface apparent emittance yields excellent agreement with the rough surface flux distributions for the large wall emittance surface.

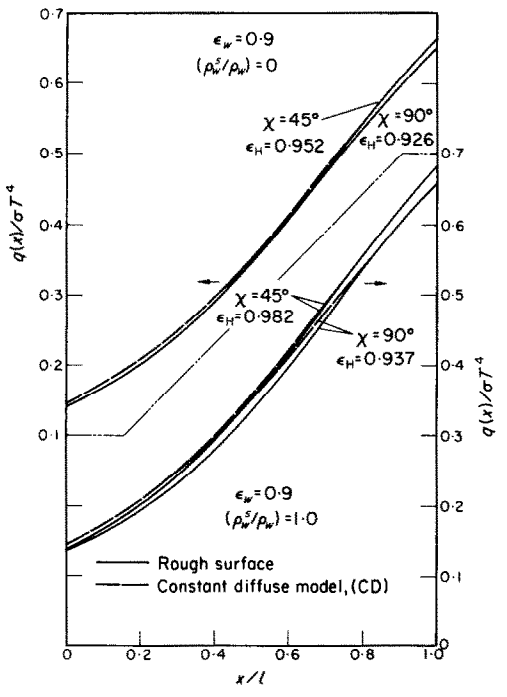

FIG. 8. Comparison of rough surface heat flux to results from simple property models ($\varepsilon_w = 0.9$).

Total heat transfer

Dimensionless total heat transfer results are presented in Table 1. As expected, the total heat transfer rate increases with increasing values for wall emittance and for identical materials, the surface with the greater surface roughness slope experiences the larger heat transfer rate. The variation of total heat transfer over the range of values considered for the surface roughness parameters is less than 10 per cent for the high emittance surface. As emittance is reduced, however, rough surface total heat transfer variation increases, finally attaining a factor of two for the low emittance surface. Again, it is of interest to evaluate the accuracy to which total heat transfer may be predicted using simple models for radiative properties. Complete disregard of roughness in CD analysis yields acceptable total heat transfer results for the high emittance surface, but the excellent agreement rapidly deteriorates as wall emittance decreases. Significant improvement is obtained when CD analysis accounts for roughness influences on hemispherical properties. All total heat transfer results for the surface with larger roughness slope are within 9 per cent of those for the rough surface. For the surface of smaller roughness slope with diffusely reflecting asperities, the maximum error in CD analysis decreases to 6 per cent. Comparable accuracy can be obtained for specularly reflecting asperities and $\chi = 90°$ only when wall emittance is used in CD analysis. Total heat transfer results obtained from DD analysis are not significantly more accurate than those calculated with the CD model.

Radiant intensity

Representative dimensionless intensity distributions are illustrated in Fig. 9 near the midpoint of the low emittance surface with the smaller roughness slope. Results are displayed for diffusely reflecting ($\rho_w^S/\rho_w = 0$) and specularly reflecting ($\rho_w^S/\rho_w = 1.0$) roughness elements as well as for the CD and CS property models employing rough surface apparent emittance.

Table 1. Dimensionless total radiant heat transfer, $(Q/l)/\sigma T^4$

Wall emittance, ε_w	(ρ_w^S/ρ_w)	Rough surface	Constant properties $\varepsilon_H = \varepsilon_a$	Constant properties $\varepsilon_H = \varepsilon_w$	Directional diffuse $\varepsilon_H = \varepsilon_a$
$\gamma = 45°, \chi = 45°$					
0·1	0·0	0·1425	0·1555* 0·1761†	0·08375* 0·09057†	0·1546
	1·0	0·1506	0·1646 0·1871	0·08375 0·09057	0·1633
0·5	0·0	0·2992	0·3214 0·3509	0·2674 0·3043	0·3187
	1·0	0·3273	0·3432 0·3649	0·2674 0·3043	0·3342
0·9	0·0	0·3856	0·3742 0·3796	0·3644 0·3756	0·3734
	1·0	0·3736	0·3794 0·3816	0·3644 0·3756	0·3773
$\gamma = 45°, \chi = 90°$					
0·1	0·0	0·1015	0·1076* 0·1184†	0·08375 0·09057	0·1076
	1·0	0·07538	0·1088 0·1198	0·08375 0·09057	0·1084
0·5	0·0	0·2749	0·2917 0·3271	0·2674 0·3043	0·2913
	1·0	0·2435	0·2974 0·3320	0·2674 0·3043	0·2925
0·9	0·0	0·3632	0·3693 0·3777	0·3644 0·3756	0·3691
	1·0	0·3591	0·3714 0·3786	0·3644 0·3756	0·3686

* Diffuse reflection (CD).
† Specular reflection (CS).

Except for a skewness toward the apex, the intensity distribution for the rough surface with diffusely reflecting asperities does not differ significantly from that for the CD property model. On the other hand, the intensity distribution for the rough surface with specularly reflecting elements does not resemble to any significant degree any of the other illustrated results. For the angular range $15° \leqslant \theta \leqslant 75°$, the intensity is the rough surface apparent directional emittance while at certain other directions it is equal to the intensity of a black surface at the plate temperature. Both of these characteristics are readily interpreted in view of the geometry of the adjoint plate system and the characteristics of the specular component of bidirectional reflectance.

and roughness included angle or slope. Local flux and total heat transfer were evaluated for a range of values for each surface roughness parameter. Supplementary heat transfer results were determined from less detailed analysis utilizing the simple property models commonly employed in engineering analysis.

The following conclusions may be drawn from the radiant heat transfer results. Surface roughness effects are for the most part unimportant for high emittance materials ($\varepsilon_w \geqslant 0{\cdot}9$). The influence of surface roughness on radiant heat transfer steadily increases as material emittance values diminish. Surface roughness slope is the more dominant rough surface parameter influencing radiant transfer for low emittance materials and can alter local and

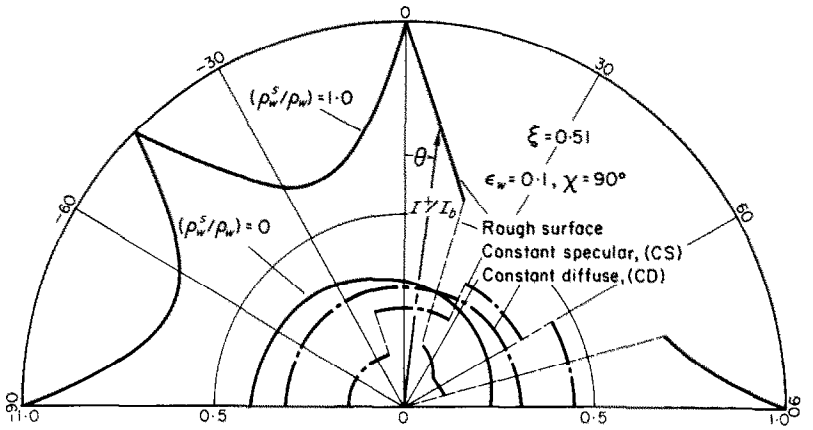

FIG. 9. Typical radiant intensity distributions ($\varepsilon_w = 0{\cdot}1$, $\chi = 90°$).

CONCLUSIONS

Radiative transfer between interacting one-dimensionally rough surfaces was formulated for a system of simple geometrical character. The direction dependent apparent thermal radiation properties of the rough surface introduced in the analysis include bidirectional reflectance and directional emittance. These rough surface properties depend on three surface roughness parameters; constituent material emittance, roughness element specularity

total heat transfer rates by a factor of two. Of the simple surface property models considered, rough surface local and total heat transfer were generally approximated most accurately by the diffuse emission–diffuse reflection model employing rough surface apparent emittance for hemispherical emittance. The error incurred in using this model to evaluate local flux for low to intermediate values of emittance, however, can be as large as 50 per cent.

REFERENCES

1. R. G. HERING and T. F. SMITH, Apparent radiation properties of a rough surface, *AIAA Paper No.* 69–622, presented at AIAA Fourth Thermophysics Conference, June 1969.
2. J. R. SCHORNHORST and R. VISKANTA, Effect of direction and wavelength dependent surface properties on radiant heat transfer, *AIAA Jl* **6**, 1450–1455 (1968).
3. J. S. TOOR and R. VISKANTA, A numerical experiment of radiant heat interchange by the Monte Carlo method, *Int. J. Heat Mass Transfer* **11**, 883–897 (1968).
4. A. F. HOUCHENS and R. G. HERING, Bidirectional reflectance of rough metal surfaces, *AIAA Progress in Astronautics and Aeronautics: Thermophysics of Spacecraft and Planetary Bodies*. edited by G. B. Heller, pp. 65–89, Academic, New York (1967).
5. M. W. WILDEN and C. H. TREAT, Directional effects in radiant heat transfer between pairs of simply arranged surfaces, *Technical Report ME*-34, Bureau of Engineering Research, The University of New Mexico (1968).
6. C. H. TREAT and M. W. WILDEN, Investigation of a model for bidirectional reflectance of rough surfaces, *AIAA Paper No.* 69–64 (1969).
7. K. E. TORRANCE and E. M. SPARROW, Theory for off-specular reflection from roughened surfaces, *J. Opt. Soc. Am.* **57**, 1105–1114 (1967).
8. M. PERLMUTTER and J. R. HOWELL, Angular distribution of emitted and reflected radiant energy from diffuse gray asymmetric grooves, *NASA TN D*-1987 (1963).
9. J. R. HOWELL and M. PERLMUTTER, Directional behavior of emitted and reflected radiant energy from a specular, gray, asymmetric groove, *NASA TN D*-1874 (1963).
10. W. Z. BLACK and R. J. SCHOENHALS, A study of directional radiation properties of specially prepared V-groove cavities, *J. Heat Transfer* **90**, 420–428 (1968).
11. E. M. SPARROW, J. L. GREGG, J. V. SZEL and P. MANOS, Analysis, results and interpretation for radiation heat transfer between some simply arranged gray surfaces, *J. Heat Transfer* **83**, 207–214 (1961).
12. E. R. G. ECKERT and E. M. SPARROW, Radiative heat exchange between surfaces with specular reflection, *Int. J. Heat Mass Transfer* **3**, 42–54 (1961).
13. R. G. HERING, Radiative heat exchange and equilibrium surface temperature in a space environment, *J. Spacecraft Rockets* **5**(1), 47–54 (1968).

EFFETS DE LA RUGOSITÉ DE SURFACE SUR LE TRANSPORT PAR RAYONNEMENT ENTRE DES SURFACES

Résumé—Le transport de chaleur entre des surfaces opaques en interaction est formulé pour des plaques contigües à température égale avec un profil de rugosité de surface unidimensionnel. La réflectance bidirectionnelle et l'émittance directionnelle de la surface rugueuse introduites dans l'analyse dépendent de l'émittance du matériau, de la spécularité de l'élément de rugosité et de la pente de la rugosité de surface. Les solutions numériques de l'équation intégrale déterminante pour l'intensité du rayonnement fournit le transport de chaleur local et total pour une gamme de chacun des paramètres de la surface rugueuse. Les résultats de transport de chaleur indiquent que les effets de la rugosité ne sont relativement pas importants pour des matériaux à émittance élevée tandis que pour des matériaux à faible émittance, la pente de la rugosité peut changer le flux local et le transport de chaleur total par rayonnement d'un facteur de deux. La comparaison du transport de chaleur de la surface rugueuse avec celui évalué grâce à des modèles simples de propriétés de la surface démontre la supériorité du modèle émission diffuse—réflexion diffuse employant l'émittance hémisphérique apparente de la surface. L'erreur encourue dans le flux local en utilisant ce modèle simple peut être, cependant, importante.

EINFLÜSSE DER OBERFLÄCHENRAUHIGKEIT AUF DEN WÄRMEAUSTAUSCH DURCH STRAHLUNG

Zusammenfassung—Es wird der Wärmeübergang durch graue Strahlung zwischen aneinanderstossenden Platten betrachtet. Die Oberflächen haben gleiche Temperatur und ein eindimensionales Rauhigkeitsprofil. Das in der Analyse eingeführte zweifach richtungsabhängige Reflexionsvermögen und das richtungsabhängige Emissionsvermögen der rauhen Oberfläche sind Grössen, die vom Emissionsvermögen des Materials, den Spiegeleigenschaften des Rauhigkeitselementes und der Neigung der Rauhigkeiten abhängen. Die numerische Lösung der bestimmenden Integralgleichung für die Strahlungsintensität liefert den lokalen und totalen Wärmeaustausch für einen Bereich eines jeden Parameters der rauhen Oberfläche. Die Ergebnisse zeigen, dass Rauhigkeitseffekte relativ unwichtig sind für Materialien mit hohem Emissionsvermögen, während für solche mit geringem Emissionsvermögen die Neigung der Rauhigkeiten den lokalen Fluss und den Gesamtwärmeübergang um den Faktor zwei ändern kann. Der Vergleich des Wärmeübergangs zwischen rauhen Oberflächen mit dem Ergebnis aus einfachen

Modellen der Oberflächeneigenschaften zeigt die Uberlegenheit des Modells bei dem diffuse Emission und diffuse Reflektion angenommen wird, da dabei das offensichtlich halbkugelige Emissionsvermögen berücksichtigt wird. Der Fehler, der bei Verwendung des einfachen Modells bei der Berechnung des lokalen Flusses gemacht wird, kann jedoch beträchtlich sein.

ВЛИЯНИЕ ШЕРОХОВАТОСТИ ПОВЕРХНОСТЕЙ НА ЛУЧИСТЫЙ ПЕРЕНОС ТЕПЛА МЕЖДУ НИМИ

Аннотация—Приводится постановка задачи о лучистом переносе тепла между непрозрачными близко расположенными поверхностями пластин равной температуры с одномерным профилем шероховатости поверхности. Введенные в анализ двунаправленная отражательная способность шероховатых поверхностей и направленная лучеиспускательная способность зависят от лучеиспускательной способности материала, зеркальности элемента шероховатости и наклона шероховатости поверхности. В результате численных расчетов основного интегрального уравнения для интенсивности излучения получены значения локального и полного переноса тепла для каждого диапазона параметров шероховатой поверхности. Результаты по переносу тепла свидетельствуют о том, что эффекты шероховатости не представляют существенной важности для материалов с высокой излучательной способностью, в то время как для материалов с низкой излучательной спьособностью наклон шероховатости может изменять в два раза локальный тепловой поток и полный лучистый перенос тепла. Сравнение вычисленного переноса тепла с переносом для пористых моделей поверхностей показывает некоторое преимущество диффузионной модели отражения. Однако, при использовании этой модели ошибка в значении локального теплового потока может быть значительной.